Article:

Xu, Nuo, Delius, Gustav W, Zhang, Lai et al. (2021) Spatial drivers of instability in marine size-spectrum ecosystems. Journal of Theoretical Biology. 110631. ISSN: 1943-5193

https://doi.org/10.1016/j.jtbi.2021.110631

Spatial drivers of instability in marine size-spectrum ecosystems

Nuo Xu[1], Gustav W. Delius[2], Lai Zhang[1,†] ,Uffe H. Thygesen[3,4], Ken H. Andersen[4]

[1]School of Mathematical Science, Yangzhou University, Yangzhou 225002 China
[2]Department of Mathematics, University of York, York YO10 5DD, UK
[3]Department of Applied Mathematics and Computer Science, Technical University of Denmark, Denmark
[4]Center for Ocean Life, National Institute of Aquatic Resources, Technical University of Denmark, Denmark
[†]Corresponding author, email: lai.zhang@yzu.edu.cn

Abstract： Size-spectrum models are a recent class of models describing the dynamics of a whole community based on a description of individual organisms. The models are motivated by marine ecosystems where they cover the size range from multicellular plankton to the largest fish. We propose to extend the size-spectrum model with spatial components. The spatial dynamics is governed by a random motion and a directed movement in the direction of increased fitness, which we call 'fitness-taxis'. We use the model to explore whether spatial irregularities of marine communities can occur due to the internal dynamics of predator-prey interactions and spatial movements. This corresponds to a pattern-formation analysis generalized to an entire ecosystem but is not limited to one prey and one predator population. The analyses take the form of Fourier analysis and numerical experiments. Results show that diffusion always stabilizes the equilibrium but fitness-taxis destabilizes it, leading to non-stationary spatially inhomogeneous population densities, which are travelling in size. However, there is a strong asymmetry between fitness-induced destabilizing effects and diffusion-induced stabilizing effects with the latter dominating over the former. These findings reveal that fitness taxis acts as a possible mechanism behind pattern formations in ecosystems with high diversity of organism sizes, which can drive the emergence of spatial heterogeneity even in a spatially homogeneous environment.

Keywords: Size-spectrum model, marine ecosystems, fitness-taxis, stability, diffusion, travelling patterns

Introduction

Marine ecosystems are dominated by trophic interactions where larger predators eat smaller prey. Various types of models have been developed to describe the dynamics of these ecosystems (Plagányi 2007; FAO 2008). Food-web models are a common modelling framework to depict species rich marine systems (Loeuille and Loreau 2005; Rossberg *et al*., 2008; Boit *et al*., 2012; Gomez-Canchong *et al*., 2012). While food webs can describe the complex interactions between species to a large degree, this approach cannot well account for individual trophic change during ontogeny, particularly for ecosystems with high biodiversity (Guiet *et al*., 2016). To overcome this difficulty, continuous size-structured community population models have been developed (Silvert and Platt 1980; Benoît and Rochet 2004). This type of models is based on the pioneering work of Sheldon *et al*. (1972) who first discovered that the biomass remains at a nearly constant level in logarithmically increasing size intervals, which triggered the definition of 'size spectrum' (Silvert and Platt 1978; Kerr and Dickie 2001; Benoît and Rochet 2004; Andersen and Beyer 2006, Fig.1). The size-spectrum approach redefines the marine ecosystems in terms of body size rather than biological species identity, which provides community-level predictions with relatively few model processes and assumptions (Blanchard *et al*., 2009).

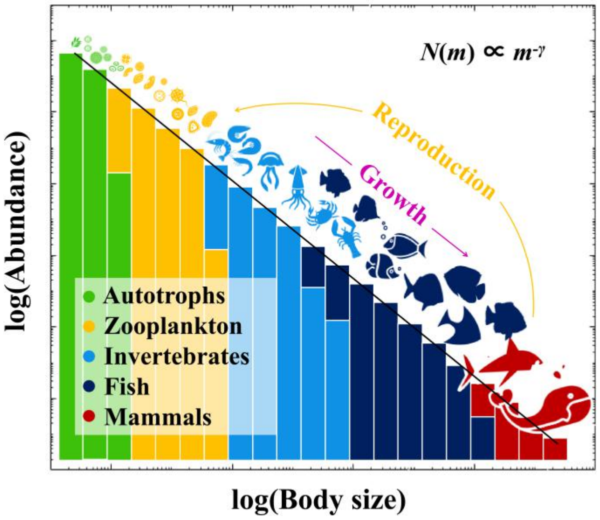

Fig. 1 Conceptual illustration of marine size spectrum extending from autotrophs to mammals in log-log axes (refined from Heneghan *et al*. (2019)). It is shown that the logarithmic abundance ($N(m)$) and logarithmic body size (m) are approximately linear with a gradient near -2 (i.e., $\gamma = 2$).

Biomass size spectra have been widely used in marine ecosystems. Here, predation is the primary process promoting the energy flow in the ecosystem, consisting of growth, mortality and reproduction (Benoît and Rochet 2004). Silvert and Platt (1978, 1980) first established the existence of a power-law steady state, which led to the practice of evaluating the state of an aquatic ecosystem by the slope and intercept of the biomass size spectrum in a log-log plot (Andersen and Beyer 2006). Blanchard *et al*. (2009) extended the model, disaggregating the ecosystem to pelagic and benthic pathways to describe the dynamics of coupled size spectra. Datta *et al*. (2010) derived the dynamic equations (the jump-growth and Mckendrick-von Foerster equations)

=from a simple stochastic process of predation, and further showed how stability of the system is affected by predator-prey mass ratio, diet breadth and feeding efficiency (Datta *et al.* 2011).

While dynamic models of community size spectra have been widely applied to understand how the abundance of predators change with body size through the size-based ontogenetic processes (Benoît and Rochet, 2004; Blanchard *et al.*, 2009; Gilljam *et al.*, 2011), the effects of organisms' movements on marine size spectrum have less been studied. Previously, a size-spectrum model accounting for advection and diffusion movements has been developed to mimic the role of top predators at a large scale of marine ecosystems (Apex Predators ECOSystem Model, in short APECOSM; Maury, 2010). This model was coupled with a biogeochemical model (The Pelagic Interaction Scheme for Carbon and Ecosystem Studies, in short PISCES, Aumont *et al.*, 2003; Aumont and Bopp, 2006) to explore the climatic responses of marine pelagic communities and it was found that spatial distribution of population biomass was significantly shaped with a substantial biomass increase for small marine organisms (Lefort *et al.*, 2015). In addition, a spatially explicit marine size spectrum was developed to explore the effects of the biotic (behavior movement, e.g. diffusion and taxis) and abiotic (passive transport, e.g. mixing) on individual growth and community structure in marine ecosystems (Castle *et al.*, 2011). Results showed that spatial distribution of different-sized organism abundance was intimately correlated with primary production.

However, to our best knowledge, there has been no attempt to explore the stability properties of marine size spectrum in a spatially explicit dynamic size-spectrum model and the potential spatial biomass patterns of different-sized individuals. We employ a marine size-spectrum model with the two spatial movements of diffusion and taxis to explore how the interplay of these spatial processes affects the stability of the marine size spectrum in a spatially homogeneous environment. While the diffusion process describes random movements, the term taxis is used to indicate directed movement as a response to environmental cues. In prey taxis, a predator moves in response to prey, so that the mean velocity of the predator is determined by the gradient of the prey density. This leads to an advection term in the equation governing the predator density, as first derived by Kareiva and Odell (1987). Ainseba *et al.* (2008) described the local interactions of species modeled by Lotka-Volterra interactions with prey-taxis and found that predators moving in the direction of higher prey concentrations would not destabilize the uniform steady state. Rather than considering completely random movements or just a response to other species, the present work takes conspecific feedback into account, that is, 'fitness taxis' termed by Heilmann *et al.* (2018), which means that population moves towards areas with high fitness, as first proposed by Cosner (2005).

The present work aims to address the question whether the spatial irregularities of marine communities can be a result of internal dynamics or must have a basis in spatial irregularities of the marine environment. To this aim, we first derive the equilibrium size-spectrum in a non-spatial marine size-spectrum model, which is also the equilibrium of the spatially augmented counterpart. Local equilibrium stability in both non-spatial and spatial models are analyzed by Fourier analysis. Finally, we carry out numerical simulations to demonstrate the emerging spatial patterns, which are non-stationary and travelling in size.

Models and methods

The model is based on the paradigm that body size is the main factor to determine individual vital rates, which in turn affect population dynamics. We take growth, mortality, and reproduction as key processes in the life history of fish individuals, where predation is a primary way to promote the energy flow in the ecosystem. We do not impose a size range for modeled organism but assume a size range from 0 to infinity. While this assumption looks unrealistic in nature, it allows our model to be scale-invariant, and allows us to perform an analytic Fourier analysis. Moreover, valuable insight into the stability effects of diffusion and fitness-taxis drawn from our model can to a large degree be translated to real ecosystems with wide size ranges. We start with a description of the model without spatial movements. For convenience, the model without spatial movements is termed a temporal size-spectrum model and the one with spatial movements as a spatio-temporal size-spectrum model. The analytic equilibrium stability analysis as well as the numerical method for finding the spatial patterns are briefly outlined at the end of this section with details being deferred to appendices.

Temporal size-spectrum model

Denote by $N(m, t)$ the abundance density of organisms with body size m (gram) at time t (year). The community size spectrum model is given by the equation

$$\frac{\partial N(m,t)}{\partial t} = -\frac{\partial}{\partial m}\left(g(N,m)N(m,t)\right) - \mu(N,m)N(m,t) + R(N,m), \tag{1}$$

where $g(N, m)$ and $\mu(N, m)$ are the growth rate (mass per time) and mortality rate (per time) of individuals with size m. $R(N, m)$ encodes the effect of population reproduction, which we will discuss further below. The growth and mortality rates are

$$g(N,m) = \alpha A m^q \int wN(w,t)\varphi(m/w)dw\,,$$

$$\mu(N,m) = \int Aw^q N(w,t)\varphi(w/m)dw + \eta\,.$$

Here, Am^q is the volumetric search rate of m-sized individuals, and η is the background mortality. We assume that the energy obtained from predation after paying metabolic costs is invested to growth and reproduction (Fig. 1). Therefore, α represents the realized growth efficiency. The integrals in the growth and mortality describe the possible encountered food and predation mortality, respectively, which depend on the size ratio between predator and prey. The definite relationship between predator and prey is specified by a log-normal size kernel

$$\varphi(m/w) = \exp\left(-\frac{\left(\log(m/w) - \beta\right)^2}{2\sigma_1^2}\right),$$

where σ_1 determines the width of the size kernel and e^β is the preferred predator-prey mass ratio (Ursin, 1973). The model (1) without the term $R(N, m)$ is the classic McKendric-von Forerster equation (Kot, 2001; Benoît and Rochet, 2004).

Since all organisms in our model have a dual trophic role: being predated by large organism and preying upon small ones, thus we cannot model the egg stage explicitly. However, it is possible to capture the main features of reproduction that are significant to the size-spectrum dynamics, that is, move down the biomass from large weight to small weight and then replenish the population numbers of small-sized individuals. Here, we model the reproduction rate $R(N, m)$ in the same way as in Capitán and Delius (2010), which is given by

$$R(N,m)=\iint\left(-B(m,w,w')N(m,t)+B(w,m,w')N(w,t)+\frac{w-w'}{m}B(w,w',m)N(w,t)\right)dwdw'. \quad (2)$$

The modelling of equation (2) is explained as follows.

It is assumed that a birth event happens from a parent organism with size w to produce small offspring with size m, which moves the parent to a lower size w' due to spawning. We set the number of offspring to be the mass ratio $(w\text{-}w')/m$ which indicates the equality between the total offspring weight and the weight lost by the parent, described by the term

$$\iint\frac{w-w'}{m}B(w,w',m)N(w,t)dwdw'. \quad (3)$$

and the term $B(w, w', m)$ indicates the birth rate from parent organisms with size w who decline in weight w' and produce offspring of size m, which can be specified as

$$B(w,w',m)=m^{-1}w'^{-1}B_0(w/w',m/w),$$

where $B_0(w/w', m/w)$ is of the following form

$$B_0(w/w',m/w)=b_0\frac{1}{\sqrt{2\pi}\sigma_\nu}\exp\left(-\frac{(\log(w/w')-\nu)^2}{2\sigma_\nu^2}\right)\frac{1}{\sqrt{2\pi}\sigma_\mu}\exp\left(-\frac{(\log(m/w)-\mu)^2}{2\sigma_\mu^2}\right).$$

This equation is basically a combination of two log-normal Gaussian functions, with the former describing an average weight reduction of the parent by a factor of e^{v} and the latter an average offspring-parent size ratio of e^{μ}.

Besides the above birth event, the abundance of m-sized population can also be increased by the reduction in weight of large-sized organisms indicated by

$$\iint B(w,m,w')N(w,t)dwdw'. \quad (4)$$

and decreased as a consequence of spawning of m-sized organisms indicated by

$$\iint -B(m,w,w')N(m,t)dwdw'. \quad (5)$$

Taken together, these three possible events (3)-(5) contribute to the reproduction term in equation (2).

Spatio-temporal size-spectrum model

We now take spatial movements into consideration. Denote by $N(m, x, t)$ the population density of organisms with size m at location x (km) and time t. Then the spatially extended size-spectrum model is given by

$$
\begin{aligned}
\frac{\partial N(m,x,t)}{\partial t} &= -\frac{\partial}{\partial m}\left(g(N,m,x)N(m,x,t)\right) - \mu(N,m,x)N(m,x,t) + R(N,m) \\
&\quad - d_0 \frac{\partial}{\partial x}\left(N(m,x,t)\frac{\partial}{\partial x}\left(m^{-1}g(N,m,x) - \mu(N,m,x)\right)\right) \\
&\quad + d_1 \frac{\partial^2 N(m,x,t)}{\partial x^2}.
\end{aligned}
\tag{6}
$$

The first row represents reaction dynamics similar to the description of the temporal model. The second row represents the spatial movements of fitness taxis, which is related to individual growth as well as mortality and depicted in the form of g/m - μ. The negative sign at the beginning expresses individuals' preference for higher fitness. The last term represents the spatial movements due to diffusion, meaning that individuals move from regions of higher density to lower density randomly. In the presence of spatial components, the growth and mortality rates are now of the forms

$$
g(N,m,x) = \alpha A m^q \iint w N(w,y,t)\varphi(m/w)\psi(x-y)\,dw\,dy\ ,
$$

$$
\mu(N,m,x) = \iint A w^q N(w,y,t)\varphi(w/m)\psi(x-y)\,dw\,dy + \eta\ .
$$

The integrals involve a spatially non-local kernel ψ,

$$
\psi(x-y) = \frac{1}{\sqrt{2\pi}\sigma_2}\exp\left(-\frac{(x-y)^2}{2\sigma_2^2}\right),
$$

where σ_2 is the width. This space kernel allows a predator to encounter prey over a spatial range close to their position rather than at the exact location of the predator (Grindrod, 1988; Banerjee and Volpert, 2016b; Malchow *et al.*, 2008).

Analytic and numerical analysis

We briefly outline the method of deriving the equilibrium size spectrum to the temporal model (Appendix A), and the method of performing local stability analysis around the equilibrium for the temporal model (Appendix B) as well as for the spatio-temporal model (Appendix C). The numerical algorithm for illustrating the spatial patterns is summarized in Appendix D. Detailed mathematical computations are presented in their respective appendices. Readers who are mainly interested in the biological findings can skip this section, and directly go to the next section.

The equilibrium to the temporal model (1) is assumed to be of the power-law form, that is, $N_s(m) = N_0 m^{-\gamma}$, where N_0 is a constant, indicating the magnitude of the marine size-spectrum. For $N_s(m)$ to be an equilibrium to the temporal model, an additional assumption is imposed throughout this paper, that is, the volumetric search rate exponent q is equal to γ-1. Such an assumption enables us to obtain closed forms of integrals over unlimited size ranges (Datta *et al.*, 2011). In fact, if $\gamma = 2$, then $q = 1$, which is exactly the empirically observed value of the search rate coefficients (Andersen *et al.*, 2016). By setting $m = m_0 e^r$ and $N(m, t) = u(r, t)e^{-r}m_0^{-1}$ direct calculation yields a condition for the parameters that can be easily satisfied, for instance, under the default parameter values in Table 1 (Appendix A).

Table 1. Model parameters

Symbol	Value	Units	Interpretation
A	600	$\text{year}^{-1}\text{g}^{-q}$	Coefficient of feeding rate[1]
β	log(100)	-	Nature log of preferred predator-prey mass ratio[2]
σ_1	1.5	-	Width of size-selection function[3]
σ_2	1	-	Width of space-selection function[4]
q	0.8	-	Exponent of volumetric search rate[5]
γ	1.8	-	Marine size spectrum exponent[5]
α	0.4	-	Growth efficiency[6]
μ	-8	-	Nature log of offspring-parent mass ratio[7]
σ_μ	1.5	-	Variance in offspring-parent mass ratio[8]
v	0.2	-	Natural log of parent weight before/after reproduction[7]
σ_v	0.05	-	Variance in parent weight before/after reproduction[7]
η	0.1	year^{-1}	Background mortality rate[9]
b_0	1	year^{-1}	Coefficient of reproduction rate[10]
m_0	1	g	Reference weight[11]
d_0	varied	km^2	Coefficient of the fitness taxis
d_1	varied	$\text{km}^2\ \text{year}^{-1}$	Coefficient of the diffusion

[1] Plank and Law (2011);

[2] Ursin (1973); Jennings *et al.* (2001);

[3] Datta *et al.* (2011);

[4] Heilmann *et al.* (2018);

[5] Andersen and Beyer (2006); Plank and Law (2011); Hartvig *et al.* (2011); q is always set to equal γ-1.

[6] Zhang *et al.* (2013).

[7] Capitán and Delius (2010);

[8] Adjusted to result in stability of both temporal and spatio-temporal size-spectrum model.

[9] Datta *et al.* (2010); Rochet and Benoît (2011);

[10] Normalized reproduction rate, conclusion is not sensitive to this parameter .

[11] Selected to make the fish size-range reasonable in numerical simulations (e.g. Fig. 2B);

We perform the local stability analysis of the power-law equilibrium $N_s(m)$ for the temporal model using Fourier analysis (Appendix B). To this end, we first transform the model (1) translation-invariant form by setting $v(r, t) = e^{qr}u(r, t)$, and then Fourier expand the scaled population density, that is, $v(r, t) = \int e^{ikr}a(k, t)dt$ where $a(k, t)$ are the Fourier coefficients with k being the wave number in the direction of logarithmic body size. Substituting the Fourier expansion into the translation-invariant system yields a system of differential equations for the Fourier coefficients $a(k, t)$. Finally, we linearize this system around the steady state to obtain the eigenvalue function against the wave number k, which allows us to determine the stability of the power-law equilibrium. Analogously, we can perform stability analysis of the power-law equilibrium in the spatio-temporal model and derive the eigenvalue function against the size wave number k and space wave number l (Appendix C).

We also use Fourier methods to perform numerical simulations of the temporal and the spatio-temporal model (Appendix D). To be able to employ Fourier series, we impose periodic boundary conditions on size and space. While there is no biological motivation for this, the solutions are not strongly dependent on the length of the size and space domain as long as they are sufficiently large (e.g., sufficiently larger than the nature log of the preferred predator-prey mass ratio). We numerically solve the resulting system of ordinary differential equations for the Fourier coefficients (i.e., $a(k, t)$). Applying the inverse Fourier analysis to those Fourier coefficients, we obtain time-series solutions for the population biomass density $u(r, x, t)$. Default parameter values are summarized in Table 1.

Results

Figure 2A demonstrates the real part of the eigenvalue $\lambda(k)$ as a function of the size wave number k for two cases: stable equilibrium under the default parameter values in Table 1 (dashed curve), and the unstable equilibrium with a slight different parameter setting (solid curve). In case of the unstable equilibrium, exciting the most unstable mode (approximately $k = 82$) yields a travelling solution (Fig. 2B).

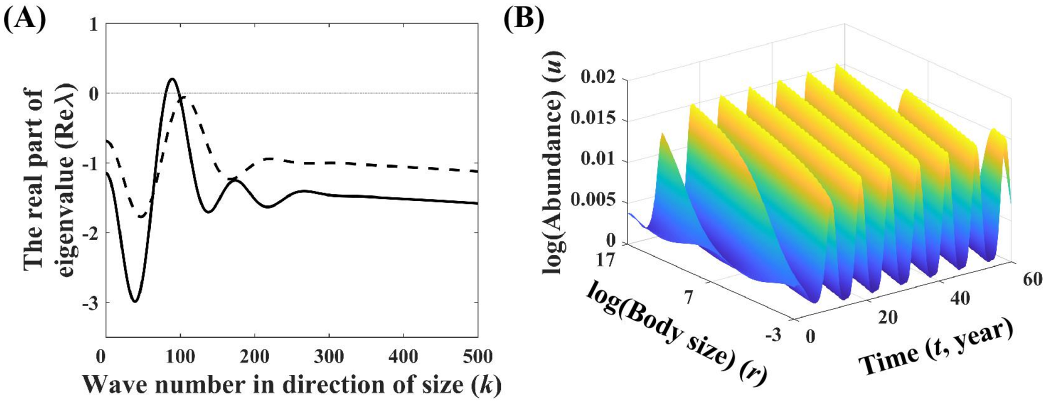

Fig. 2 For the temporal model (1): (A) Real part of the eigenvalues $\lambda(k)$ against wave numbers in the direction of size k, and (B) the travelling wave solution of log-form abundance $u(r, t)$ for logarithmic body size r and time t. Parameters for the stable equilibrium are listed in Table 1, and for the unstable equilibrium are the same as default except for nature log offspring:parent mass ratio $\mu = -10$.

When spatial processes are taken into account, we are primarily interested in how diffusion and fitness-taxis interact to affect equilibrium stability in the spatio-temporal model (3). Clearly, the equilibrium of the temporal model remains the equilibrium of the spatio-temporal model. Here we focus on the stable equilibrium size spectrum in Fig.2A. Given a pair of the coefficients of diffusion (d_1) and taxis (d_0), Figure 3A illustrates the unstable modes in the space spanned by the size wave number k and the space wave number l. The figure shows that there exists unstable modes, which will result in spatially inhomogeneous distribution of population densities when these unstable modes are excited. Figure 3B shows the emerging spatial patterns when the most unstable mode is triggered, which is non-stationary, travelling in time (Fig. 3C) but periodic in space (Fig. 3D).

To disentangle the role of diffusion and fitness-taxis in the equilibrium stability, we vary both coefficients of diffusion (d_1) and fitness taxis (d_0) (Fig. 4A). Clearly, fitness taxis favors the emergence of spatial patterns whereas diffusion prevents patterns (also see Appendix C for analytic analysis). Interestingly, these two effects are strongly asymmetric given the same strength (i.e., $d_0 = d_1$), and the stabilizing effect dominates over the other. Surprisingly, with increasing taxis strength, the unstable region in the wave number k-l space does not always expand, but approaches a limit in both size and space directions. Analytic analysis reveals that the saturation is due to the nonlinear interaction between fitness taxis induced instability and diffusion induced stability (Appendix E).

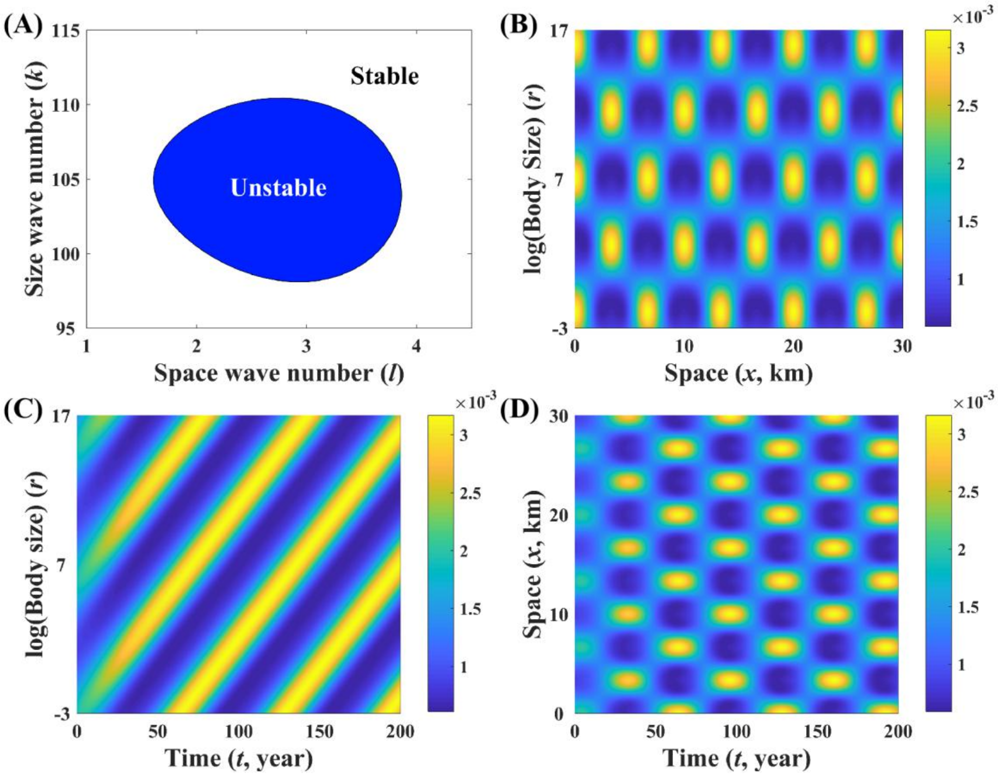

Fig. 3 (A) The unstable modes in the k-l wave number space, (B) the emerging spatial pattern, and (C) time evolution with fixed space position and (D) size. Parameters are listed in Table 1, and the coefficients of diffusion and fitness are respectively $d_1 = 0.1$ and $d_0 = 1.5$.

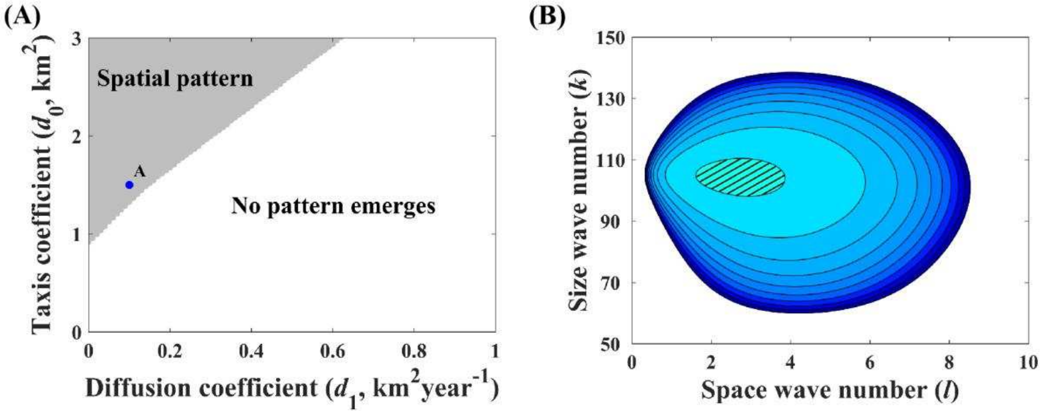

Fig. 4 (A) Diagram of spatial patterns in the space spanned by diffusion (d_1) and fitness taxis (d_0) coefficients, and (B) the evolution of region with unstable modes in the *k*-*l* wave number space with increasing taxi strength ($d_0 \in [1.5, 15]$ increases with deepening blue color) but fixed diffusion ($d_1 = 0.1$). The blue point **A** in (A) corresponds to Fig. 3 and the shaded grid area in (B) corresponds to Fig. 3A. Parameters are listed in Table 1.

When the widths of the size and space kernel are varied, we see that wider kernels favor equilibrium stability in the spatio-temporal model (Fig. 5). The difference is that the size kernel width primarily affects the unstable modes in the size direction, while the space kernel width affects the unstable modes in the space direction. Moreover, narrower size kernel width allows more unstable size modes, and even makes the equilibrium unstable.

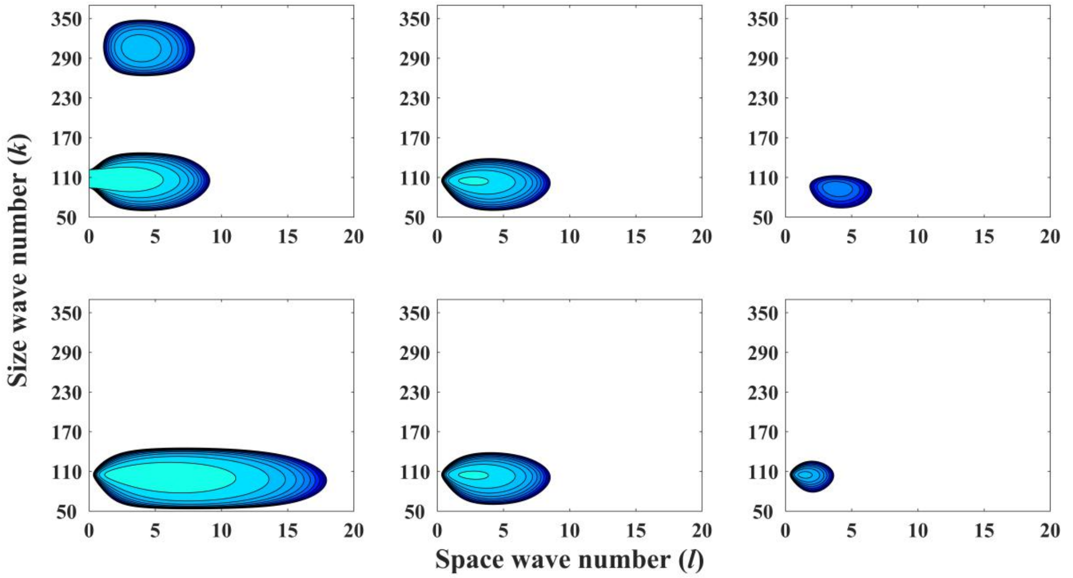

Fig. 5: The evolution of region with unstable modes in the *k*-*l* wave number space with intensified taxi strength ($d_0 \in [1.5, 15]$ increases with deepening blue color), and fixed diffusion ($d_1 = 0.1$). Top panels correspond to the width of size kernel σ_1: 0.5 (left), 1.5 (middle) and 3 (right), and the bottom panels correspond to the width of the space kernel σ_2: 0.5 (left), 1 (middle) and 2 (right). Other parameters are listed in Table 1.

Discussion

We have developed a spatially augmented marine size-spectrum model to explore the stability properties of equilibrium solutions, where animals move both randomly and towards higher population fitness. Previously, several models have considered spatial movements (i.e., diffusion and advection) in a size-spectrum framework, such as the APECOSM model (Maury, 2010), the COBALT model (The Carbon, Ocean Biogeochemistry and Lower Trophics marine ecosystem model; Stock *et al.*, 2014; Waston *et al.*, 2015), the PISCES model (Aumont *et al.*, 2003; Aumont and Bopp, 2006; Lefort *et al.*, 2015). However, these models were generally studied in an applied context. To our best knowledge, the present work is the first theoretical attempt to investigate equilibrium stability in a spatially explicit marine size-spectrum model.

Population fitness in our model is measured by the proxy $g/m - \mu$, which integrates the gain of food and losses to predation. Positive fitness indicates that the environment benefits an animal's population growth, and thus appeals to individuals, while negative fitness implies a harsh environment in which individuals would try to avoid foraging. An alternative fitness proxy can be of the form $(g/m)/\mu$, which is the well-known Gilliam's rule (Gilliam and Fraser 1987). This fitness proxy tends to optimize an individual reproductive output of its whole life. While both fitness proxies have been widely employed in the literature (Abrams 1990; Visser 2007; Kiørboe *et al.*, 2017; Heilmann *et al.*, 2018), we adopted the first fitness proxy mainly because it is analytically tractable, but it would be interesting to see the impacts of the other fitness proxy on equilibrium stability.

The spatial foraging kernel was introduced to overcome the ill-posedness of the problem, a similar issue to which was encountered by Heilmann *et al.* (2018). In the absence of this spatial kernel short-wave disturbances increase exponentially. In the presence of the spatial kernel, short-wave perturbations decay exponentially, and the unstable wave modes first grow exponentially but ultimately become saturated (Appendix F). In the present work, the spatial foraging kernel stabilizes the equilibrium with wider kernel favoring stability (Fig. 5). Such a spatial foraging kernel has been demonstrated in non-structured prey-predator models to exhibit a stabilizing effect (Banerjee and Zhang 2016), as well as a destabilizing effect if the kernel width exceeds a threshold value (Pal *et al.*, 2019); however, the later effect is not observed in our model.

The reproduction process plays a stabilizing role. This process and predation act as the two driving forces that propagate the energy flux through the whole ecosystem. In the absence of the reproduction process, we found that the predation process always makes the equilibrium solution unstable in the temporal model (Datta *et al.*, 2011). The reproduction term enabled us to find a stable equilibrium solution and then made it possible to understand how different scales of space and size perturbations affect the spatio-temporal dynamics. Most exiting studies of equilibrium stability of size-spectrum models employed the predation process as the sole driving force, ignoring the reproduction process (Benoît and Rochet 2004; Datta *et al.*, 2010, 2011; Plank and Law, 2011). This is mainly because the egg stage cannot be explicitly modeled since every individual in size-spectrum models is assumed to grow by predating on smaller organisms, whereas eggs of course do not predate. Our modeling of population reproduction originated from Capitán and Delius (2010), who studied the size-spectrum stability in a scale-invariant model for marine population dynamics where reproduction was developed based on a Markov chain, and reported that the reproduction stabilized equilibrium. Alternatively, a stable equilibrium might arise in a truncated size spectrum by limiting organisms' size to a finite range and imposing a constant biomass for the organism with the smallest body size (Benoît and Rochet 2004).

The two spatial processes of diffusion and fitness-taxis have contrasting roles in determining equilibrium stability. While diffusion always stabilizes equilibrium (Appendix C), fitness-taxis can destabilize it (Fig. 3A). In the latter case, non-stationary patterns emerge that are travelling in size and periodic in space (Fig. 3B, 3C, 3D). Previously, Heilmann *et al.* (2018) considered a two-species model with diffusion and fitness-taxis as well as spatial kernel, and found a variety of spatial patterns including stationary spatial patterns, standing and travelling waves, and chaotic spatio-temporal patterns. We did not observe stationary patterns nor chaotic patterns in our model, but we did observe travelling waves for certain parameter values (Appendix G). The diverse patterns in Heilmann *et al.* (2018) are due to the taxis-driven instability as well as taxis-diffusion driven instability, the latter of which is basically the same as the classic Turing mechanism (Turing 1952), but is impossible to occur in our model. This is because our model fundamentally differs from two-species predator-prey model in the way population abundance changes. In particular, our model takes the growth of individuals and the resulting ontogenetic diet shift into account. This size-spectrum approach makes our study unique in the context of pattern formation in ecosystems with organisms of diverse sizes.

While we have revealed fitness-taxis to be a significant mechanism for creating spatial patterns in marine ecosystems, the unstable modes in the wave number *k*-*l* space were constrained to a finite region (Fig. 5), which did not always expand, but instead approached a limit in both directions of size and space as taxis strength is continuously intensified (i.e., d_0). This is due to the nonlinear interactions between taxis-induced instability and diffusion-induced stability (Appendix E). Moreover, the region with unstable modes decreased with increasing width in the size and spatial kernels (Fig. 5), suggesting that foraging kernels with large widths promote ecosystem stability. Note that all individuals in our model have exactly the same diffusion rate, taxis strength, size and space foraging kernel width, meaning that these factors are all size-independent. Since it is reasonable to assume that large individuals own large rates in diffusion as well as in taxis strength (Castle *et al*., 2011), or wide size and space width (Kramer and Chapmanm 1999; Haskell *et al*., 2002; Jetz *et al*., 2004, Nash *et al*., 2013), a particularly interesting and ecological relevant question arises what happens to the marine spatio-temporal dynamics if these factors are size-dependent. Zhang *et al*. (2014) considered a size-structured population model where diffusion rate increased allometrically with body size and found that the size-dependent diffusion promoted the emergence of spatial patterns, specifically, chaotic patterns. However, adding size-dependency either in diffusion, fitness taxis, size or spatial kernels to our model will break scale-invariance, hence making our model analytically intractable. Nonetheless, considering the size-dependency will be a promising future work.

Our finding that fitness-taxis promotes spatial patterns in marine ecosystems has important biological significance. In general, marine ecosystems are constantly exposed to changes from natural or anthropogenic origins, and these changes may alter population fitness, creating fitness gradients and thus directing organism movements. For instance, fisheries create a harsh environment for targeted fishes, which will lower their fitness and thus drive them away from regions with heavy fishing pressure. Marine ecosystems are also substantially impacted by human pollution (Votier *et al.*, 2005, 2008), which may provide a considerable amount of nutrient inputs. The supplement of nutrients can attract epipelagic and migratory communities (Maury, 2010) for the reason of enhanced fitness. Growing evidence suggests the accelerated global warming trends by human activities may cause an average of 1.3-1.8°C increase by the mid-century (2046-2065; IPCC, 2007). Empirical studies showed that elevated temperature benefits foraging rate but also burdens metabolic costs, thus altering population fitness (Fry, 1971; Sandersfeld *et al.*, 2015). Thus, global warming could be an important environmental forcing driving spatial heterogeneity of marine organism's abundance distribution (Beaugrand *et al.*, 2009, McGinty *et al.*, 2011) possibly through the spatial movement of fitness-taxis.

In conclusion, we studied the stability properties in a spatially explicit marine size-spectrum model with diffusion and fitness-taxis. While diffusion always stabilizes the equilibrium, fitness-taxis can destabilize it, leading to spatially inhomogeneous population densities that travel in size. These findings suggest that fitness-taxis serves as a possible mechanism underlying marine spatial pattern formations. An interesting future work is how this mechanism will be reinforced by environmental factors that can potentially alter population fitness. Moreover, since our model is purely size-based ignoring species identity, a promising future work is to explicitly address the spatio-temporal dynamics of species-rich ecosystems with species-based network approaches.

Author contributions: KHA, UHT, GWD and LZ developed the model. NX, LZ and GWD carried out the analytical analysis, and performed the numerical simulations and wrote the manuscript draft. All authors contributed to discussion of results and the final text.

Acknowledgements: LZ was financially supported by the NSF of China (11871065), the NSF of Jiangsu Province (BK20181450), by the Jiangsu Distinguished Professor Program, and the Yangzhou Talent Program of 'LvYangJinFeng'. KHA and UHT were supported by The Centre for Ocean Life, a Villum Kahn Rasmussen Centre of Excellence funded by the Villum Foundation.

References

Abrams M. D., 1990. Adaptations and responses to drought in Quercus species of North America. *Tree Physiology* 7, 227-238.

Ainseba D., Bardahmane M., Noussair A., 2008. A reaction-diffusion system modeling predator-prey with prey-taxis. *Nonlinear Analysis: Real World Applications* 9, 2086-2105.

Andersen K. H., Berge T., Gonçalves R. J., Hartvig M., Heuschele J., Hylander S., Jacobsen N. S., Lindemann C., Martens E.A., Neuheimer A. B., Olsson K., Palacz A., Prowe F., Sainmont J., Traving S. J., Visser A.W., Wadhwa N., Kiørboe T., 2016. Characteristic Sizes of Life in the Oceans, from Bacteria to Whales. *Annual Reviews in Marine Science* 8, 217-241.

Andersen K. H., Beyer J. E., 2006. Asymptotic body size determines species abundance in the marine size spectrum. *American Naturalist* 168, 54-61.

Aumont O., Maier-Reimer E., Blain S., Monfray P., 2003. An ecosystem model of the global ocean including Fe, Si, P colimitations. *Global Biogeochemical Cycles* 17, 1060.

Aumont O., Bopp L., 2006. Globalizing results from ocean in situ iron fertilization studies. *Global Biogeochemical Cycles* 20, 1-15.

Banerjee M., Volpert V., 2016b. Spatio-temporal pattern formation in Rosenzweig–MacArthur model: effect of nonlocal interactions. *Ecological Complexity* 30, 2-10.

Banerjee M., Zhang L., 2016. Stabilizing role of nonlocal interaction on spatio-temporal pattern formation. *Mathematical Modelling in Natural Phenomenon* 11, 103-118.

Beaugrand G., Luczack C., Edwards M., 2009. Rapid biogeographical plankton shifts in the North Atlantic Ocean. *Global change biology* 15, 1970-1803.

Benoît E., Rochet M. J., 2004. A continuous model of biomass size spectra governed by predation and the effects of fishing on them. *Journal of Theoretical Biology* 226, 9-21.

Blanchard J. L., Jennings S., Law R., Castle MD., McCloghrie P., Rochet, M. J., Benoît E., 2009. How does abundance scale with body size in coupled size-structured food webs? *Journal of Animal Ecology* 78, 270-280.

Boit A., Martinez N.D., Williams R.J., Gadeke U., 2012. Mechanistic theory and modelling of complex food-web dynamics in Lake Constance. *Ecology Letters* 15, 594-602.

Capitán J. A., Delius G. W., 2010. Scale-invariant model of marine population dynamics. *Physical Review E* 81, 061901.

Castle M. D., Blanchard J. L., Jennings S., 2011. Predicted effects of behavioural movement and passive transport on individual growth and community size structure in marine ecosystems. *Advances in Ecological Research* 45, 41-66.

Cosner C., 2005. A dynamic model for the ideal-free distribution as a partial differential equation. *Theoretical Population Biology* 67, 101-108.

Datta S., Delius G. W., Law R., 2010. A jump-growth model for predator-prey dynamics: derivation and application to marine ecosystems. *Bulletin of Mathematical Biology* 72, 1361-1382.

Datta S., Delius G. W., Law R., Plank M. J., 2011. A stability analysis of the power-law steady state of marine size spectrum. *Journal of Mathematical Biology* 63, 779-799.

FAO, 2008. Fisheries management. 2. The ecosystem aproach to fisheries. 2.1 Best practices in ecosystem modelling for informing and ecosystem aproach to fisheries. FAO Technical Guidelines for Responsible Fisheries, 4.

Fry F. E. I., 1971. Fish Physiology Vol. VI Environmental Relations and Behavior (eds Hoar, W. S. & Randall, D. J.), 1-99.

Gilliam J. F., Fraser D. F., 1987. Habitat selection under predation hazard: test of a model with foraging minnows. *Ecology* 68, 1856-1862.

Gilljam D., Thierry A., Figueroa D., Jones I., Lauridsen R., Petchey O., Woodward G., Ebenman B., Edwards F. K., Ibbotson A. T. J., 2011. Seeing double: Size-based versus taxonomic views of food web structure. *Advances in Ecological Research* 45, 67-133.

Gomez-Canchong P., Quinones R. A., Brose U., 2012. Robustness of size-structure across ecological networks in pelagic systems. *Theoretical Ecology* 6, 45-56.

Grindrod P., 1988. Models of individual aggregation or clustering in single and multi-species communities. *Journal of Mathematical Biology* 26, 651–660.

Guiet J., Poggiale J. C., Maury O., 2016. Modelling the community size-spectrum: recent developments and new directions. *Ecology Modelling* 337, 4-14.

Hartvig M., Andersen K. H., Beyer J. E., 2011. Food web framework for size-structured populations. *Journal of Theoretical Biology* 272, 113-122.

Haskell J., Ritchie M., Olff H., 2002. Fractal geometry predicts varying body size scaling relationships for mammal and bird home ranges. *Nature* 418, 527-530.

Heneghan R. F., Hatton I. A., Galbraith E. D., 2019. Climate change impacts on marine ecosystems through the lens of the size spectrum. *Emerging Topics in Life Sciences* 3, 233-243.

Heilmann I. T., Thygesen U. H., Sϕrensen M. P., 2018. Spatio-temporal pattern formation in predator-prey systems with fitness taxis. *Ecology Complexity* 34, 44-57.

IPCC, 2007. Climate change 2007: the physical science basis. In: Solomon S., Qin D., Jackson R. B., Carpenter S. R., Dahm C. N., McKnight D. M., Naiman R. J., Postel S. L., Running S. W., 2001. Water in a changing world. *Ecology Applied* 11, 1027-1045.

Jennings S., Pinnegar J. K., Polunin N. V. C., Boon T. W., 2001. Weak cross-species relationships between body size and trophic level belie powerful size-based trophic structuring in fish communities. *Journal of Animal Ecology* 70, 934-944.

Jetz W., Carbone C., Fulford J., Brown J. H., 2004. The scaling of animal space use. *Science* 306, 266-268.

Kareiva P., Odell G., 1987. Swarms of predators exhibit ‘preytaxis’ if individual predators use area-restricted search. *American Naturalist* 130, 233-270.

Kerr S. R., Dickie L. M., 2001. The biomass spectrum: a predator-prey theory of aquatic production. Columbia University Press, New York.

Kiørboe T., Saiz E., Tiselius P., Andersen K. H., 2017. Adaptive feeding behavior and functional responses in zooplankton. *Limnology and Oceanography* 63, 308-321.

Kot M., 2001. Elements of Mathematical Ecology. Cambridge University Press, Cambridge.

Kramer D., Chapmanm M., 1999. Implications of fish home range size and relocation for marine reserve function. *Environmental Biology of Fishes* 55, 65-79.

Lefort S., Aumont O., Bopp L., Arsouze T., Gehlen M., Maury O., 2015. Spatial and body-size dependent response of marine pelagic communities to projected global climate change. *Global Change Biology* 21, 154-164.

Loeuille N., Loreau M., 2005. Evolutionary emergence of size-structured food webs. *Proceedings of The National Academy of Sciences of the United States of America* 102, 5761-5766.

Malchow H., Petrovskii S. V., Venturino E., 2008. Spatio-temporal Patterns in Ecology and Epidemiology: Theory, Models, and Simulation. Chapman & Hall/CRC London.

Maury O., 2010. An overview of APECOSM, a spatialized mass balanced 'Apex Predators ECOSystem Model' to study physiologically structured tuna population dynamics in their ecosystem. *Progress In Oceanography* 84, 113-117.

McGinty N., Power A. M., Johnson M. P., 2011. Variation among northeast Atlantic regions in the response of zooplankton to climate change: not all areas follow the same path. *Journal of Experimental Marine Biology and Ecology* 400, 120-131.

Nash K. L., Graham N., Bellwood D. R., 2013. Fish foraging patterns, vulnerability to fishing and implications for the management of ecosystem function across scales. *Ecosystems* 16, 478-490.

Pal S. Ghorai S., Barnerjee M., 2019. Effects of kernels on spatio-temporal patterns of a nonlocal prey predator model. *Mathematical Biosciences* 310, 96-107.

Plagányi E. E., 2007. Models for an ecosystem approach to fisheries. Technical Reports. Rome, Italy.

Plank M. J., Law R., 2011. Ecological drivers of stability and instability in marine ecosystems. *Theoretical Ecology* 5, 465-480.

Rochet N. J., Benoît E., 2011. Fishing destabilizes the biomass flow in the marine size spectrum. *Proceedings of the Royal Society of London* 279, 284-292.

Rossberg A. G., Ishi R., Amemiya T., Itoh K., 2008. The top-down mechanism for body-mass-abundance scaling. *Ecology* 89, 567-580.

Sandersfeld T., Davison W., Lamare M. D., Knust R., Richter C., 2015. Elevated temperature causes metabolic trade-offs at the wholeorganism level in the Antarctic fish *Trematomus bernacchii*. *The Journal of Experimental Biology* 218, 2373-2381

Sheldon R. W., Prakash A., Sutcliffe Jr W. H., 1972. The size distribution of particles in the ocean. *Limnology and Oceanography* 17, 327-340.

Silvert W., Platt T., 1978. Energy flux in the pelagic ecosystem: a time-dependent equation. *Limnology and Oceanography* 23, 813-816.

Silvert W., Platt T., 1980. Dynamic energy-flow model of the particle size distribution in pelagic ecosystems. Evolution and ecology of zooplankton communities. Special symposium, vol. 3, 754-763. Hanover, NH: University Press of New England.

Stock C. A., Dunne J. P., Jasmin J., 2014. Global-scale carbon and energy flows through the marine food web: an analysis with a coupled physicalbiological mode. *Progress in Oceanography* 120, 1-28.

Turing A. M., 1952. The Chemical Basis of Morphogenesis. *Philosophical Transactions of the Royal Society of London. Series B* 237, 37-72.

Ursin E., 1973. On the prey size preferences of cod and dab. *Meddelelser fra Dammarks Fiskeriog Havundersϕgelser* 7, 84-98.

Visser, A. W., 2007. Motility of zooplankton: Fitness, foraging and predation. *Journal of Plankton Research* 29, 447–461.

Votier S. C., Hatchwell B. J., Beckerman A. P., McCleery R. H., Hunter F. M., Pellat J., Trinder M., Birkhead T. R., 2005. Oil pollution and climate have wide-scale impacts on seabird demographics. *Ecology Letters* 8, 1157-1164.

Votier S. C., Birkhead T. R., Oro D., Trinder M., Grantham M. J., Clark J.A., McCleery R. H., Hatchwell B. J., 2008. Recruitment and survival of immature seabirds in relation to oil spills and climate variability. *Journal of Animal Ecology* 77, 974-983.

Waston J. R., Stock C. A., Sarmiento J. L., 2015. Exploring the role of movement in determining the global distribution of marine biomass using a coupled hydrodynamic - Size-based ecosystem model. *Progress in Oceanography* 138, 521-532.

Zhang L., Thygesen U. H., Knudsen K., Andersen K. H., 2013. Trait diversity promotes stability of community dynamics. *Theoretical Ecology* 6, 57-69.

Zhang L., Hartvig M., 2014. Size-based predictions of food web patterns. *Theoretical Ecology* 7, 23-33.